Dynamics of Atmospheres and Oceans 86 (2019) 153–162

Contents lists available at ScienceDirect

Dynamics of Atmospheres and Oceans

journal homepage: www.elsevier.com/locate/dynatmoce

Dominant east-west pattern of diurnal temperature range observed across Zambia

Brigadier Libanda[a,*], Namwiinga Babra Nkolola[b], Ngonga Chilekana[c], Kelvin Bwalya[c]

[a] School of Geosciences, The University of Edinburgh, EH9 3FF, Edinburgh, United Kingdom
[b] School of Energy, Geoscience, Infrastructure and Society, Heriot-Watt University, EH14 4AS, Edinburgh, United Kingdom
[c] Ministry of Energy and Water Development, P.O. Box 53930, Lusaka, Zambia

ARTICLE INFO

Keywords:
Diurnal temperature range
Climate change
Cloud cover
Rainfall
Zambia

ABSTRACT

Diurnal temperature range (DTR) is an important index for climate because of its statistical relationships to greenhouse gases, urban heat, cloud cover, land use change, and aerosol haze layers. This study examines DTR trends across Zambia for the period 1930–2016 using the latest version of high-resolution monthly data (CRU TS v4.01) from the Climatic Research Unit. Non-parametric trend analyses were extensively employed at different spatial and temporal scales to quantify DTR changes. Taken together, results show a dominant east-west pattern with higher DTR values being observed in the western half of the country. Although there are noticeable differences in the magnitude from one month to the other, this east-west pattern is persistent throughout all the months. It is also found that mean annual DTR is negatively correlated with mean annual cloud cover with a strong and statistically significant coefficient of -0.8 but its correlation with precipitation weakens to -0.5 at the α 0.05. Results from the Mann-Kendall trend test shows marginal increments in DTR during all the seasons and they are all statistically significant at the α 0.05. The observed increments can be attributed to a general decrease in cloud cover over Zambia.

1. Introduction

Climate is a complicated system influenced by myriad external forcing mechanisms. Therefore, understanding its variability and change requires the use of multiple metrics. Given the influence that maximum and minimum temperatures exert on mean temperature, the use of diurnal temperature range (DTR) is an important input to climate change measures (Braganza et al., 2004; Sun et al., 2006; Qu et al., 2014). Changes in DTR can be explained by urban warming (IPCC, 2001), variations in land use/land cover (Collatz et al., 2000; Kalnay and Cai, 2003), and cloud cover (Wang and Shilenje, 2017) among others.

In many places across the globe, DTR has decreased steadily. For example, downward trends have been observed across the continental United States (Karl et al., 1991; Qu et al., 2014), in the upper Tapi Basin of India (Sharma et al., 2018) and in Europe (Makowski et al., 2009). The global downward trend of DTR was also used in the Intergovernmental Panel for Climate Change (IPCC)'s first assessment report as a substantial indicator of a warming climate exacerbated by human influences. Emitted greenhouse gases from anthropogenic activities destabilize the earth's energy budget by blocking and reflecting outgoing longwave radiation thereby raising minimum temperatures and consequently DTR (IPCC, 2007).

While there is evidence of reductions in DTR across global datasets, the need to investigate DTR trends at local and regional scales

* Corresponding author.
E-mail address: brigadier.libanda@ed.ac.uk (B. Libanda).

https://doi.org/10.1016/j.dynatmoce.2019.05.001
Received 27 December 2018; Received in revised form 29 April 2019; Accepted 1 May 2019
Available online 01 May 2019

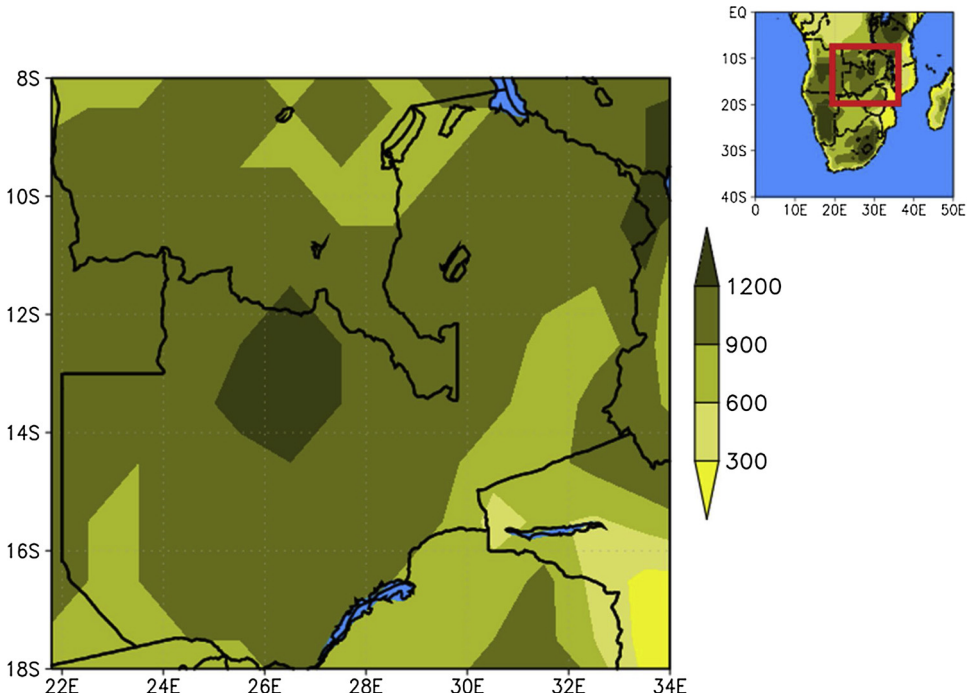

Fig. 1. Area of study showing the topographic elevation in meters above sea level based on data from Hastings and Paula (1999). Areas shaded blue are the major water bodies in the region. Insert shows the location of Zambia in southern Africa (For interpretation of the references to colour in this figure legend, the reader is referred to the web version of this article).

remain imperative because global studies are usually too coarse in scale and do not consider the local or regional factors influencing DTR. For effective formulation of climate change adaptation strategies, this study, cautions against generalizations of global trends to local and/or regional scales; this is also highlighted by the IPCC (IPCC, 2007).

Although many studies on DTR have been done in different countries, no published literature exist for the case of Zambia. Therefore, DTR variability across the country remains unknown. The goal of this study is, for the first time, to investigate the spatial and temporal distribution of DTR across Zambia. Fig. 1 presents the geographical location of Zambia in southern Africa. The topographic map shows that much of the landmass is high and flat hence best described as a plateau (Libanda and Chilekana, 2018). The climate is bimodal with a wet season running from October – April and a dry season spanning from May – September (Libanda et al., 2018).

Section 2 of this paper introduces the data and methodology used to spatially and temporally quantify DTR over Zambia. Section 3 presents the findings and an in-depth discussion of their implications. Conclusively, a summary of this work is given in section 4.

2. Data and methodological approach

2.1. Data

A summary of the datasets used in this study is given in Table 1. Overall, these datasets are of high resolution and provide an excellent surrogate for station data especially in data scarce regions of developing countries (Awange et al., 2016). These datasets have previously successfully been used to quantify DTR across the United States (Lauritsen and Rogers, 2012) and across East Africa (Wang and Shilenje, 2017).

Table 1
Summary of datasets the used in this study.

Dataset	Source	Resolution	Period used
Cloud cover	Harris et al. (2014)	$0.5^0 \times 0.5^0$	1930–2016
DTR	Harris et al. (2014)	$0.5^0 \times 0.5^0$	1930–2016
Maximum temperature	Harris et al. (2014)	$0.5^0 \times 0.5^0$	1930–2016
Minimum temperature	Harris et al. (2014)	$0.5^0 \times 0.5^0$	1930–2016
Precipitation	Harris et al. (2014)	$0.5^0 \times 0.5^0$	1930–2016

2.2. Methodological approach

The Mann-Kendall, a non-parametric test statistic has been used in this study after Mann (Mann, 1945) and Kendall (Kendall, 1975), to detect trends in DTR across Zambia. The hypothesis followed in this study is:

H_0 - No monotonic trend found in DTR

H_a - Monotonic trend is present in DTR

The computation of the Mann-Kendall test is mathematically given as:

$$s = \sum_{i=1}^{n-1} \sum_{j=i+1}^{n} sig(x_i - x_j) \tag{1}$$

From this formula, n is the sample size X_i and X_j are sequential values of X and *sig* is:

$$sig(x)\{\begin{cases} 1 & if\ x > x_i \\ 0 & if\ x = x_i \\ -1 & if\ x < x_i \end{cases} \tag{2}$$

From Eq. (1), the variance of S is given as:

$$VAR(S) = \frac{1}{18}[n(n-1)(2n+5) - \sum_{p-1}^{g} t_p(t_p - 1)(2t_p + 5)] \tag{3}$$

Where: g is the number of tied groups, n is the number of data points and t_p is the number of observations in the p^{th} group. The parameters s and n are used to investigate the significance of the trend which is associated with the Z value. An upward trend is shown by a positive score of the Z value. Conversely, a downward trend is shown by a negative score of the Z value. Mathematically, the Z value is calculated as:

$$\begin{aligned} Z &= \frac{s-1}{\sqrt{Var(s)}} if \quad s > 0 \\ &= 0 \quad if \quad s = 0 \\ &= \frac{s+1}{\sqrt{Var(s)}} \quad if \quad s < 0 \end{aligned} \tag{4}$$

Here, if the Z value is negative and the calculated probability if more that the set level of significance (in this case 95%), the trend is taken to be negative.

Another nonparametric method (Sen's slope estimator) was used to calculate the magnitude of the observed trends in DTR. The Sen's slope calculates both the linear rate of change and associated confidence levels (Sen, 1985). It is expressed as:

$$Q = \frac{Y_{i'} - Y_i}{i' - i} \tag{5}$$

Here, Y_i ' and Y_i are the values at times i' and i, where i' is greater than i, N' is all data pairs for which i' is greater than i. Q is a slope estimate.

The sequential Mann-Kendall (M-K) test (Sneyers, 1990) was used to detect abrupt changes in DTR. This approach considers forward: *u(t)* and backward: *u'(t)* sequential statistics. It also compares the relative magnitude of data as opposed to the data values themselves. The forward sequential statistic *u(t)* is standardised with a unit standard deviation and a mean of zero. In the display of the sequential M-K test, the upper and lower confidence limits correspond to 1.96 and -1.96. When the progressive M-K values cross within the limits, it indicates a significant abrupt change at $\alpha = 5\%$. Many researchers (e.g. (Wang and Shilenje, 2017; Ongoma et al., 2017) have used this approach for abrupt change studies.

The linear relation between cloud cover, precipitation and DTR was investigated using Pearson Correlation coefficient (R). Pearson correlation is obtained by dividing the covariance of the two variables by the product of their standard deviations (Pearson, 1895). Eq. (6) shows the mathematical representation of R.

$$R = \frac{\sum_{i=1}^{n}(x_i - \bar{x}).(y_i - \bar{y})}{\sqrt{\sum_{i=1}^{n}(x_i - \bar{x})^2 . \sum_{i=1}^{n}(y_i - \bar{y})^2}} \tag{6}$$

Where x denotes DTR while y shows cloud cover or precipitation outputs. The grading of linear associations ranges from -1 to 1 with 1 denoting a perfect upward linear relation and -1 showing a downward relationship. 0 shows that there is no linear relationship.

3. Results

Fig. 2 displays the monthly climatology of DTR over Zambia for the period 1930 - 2016. What stands out from these results is a dominant east-west pattern with higher DTR values being observed in the western half of the country. Although there are noticeable differences in the magnitude from one month to the other, this east-west pattern is persistent throughout all the months. The higher

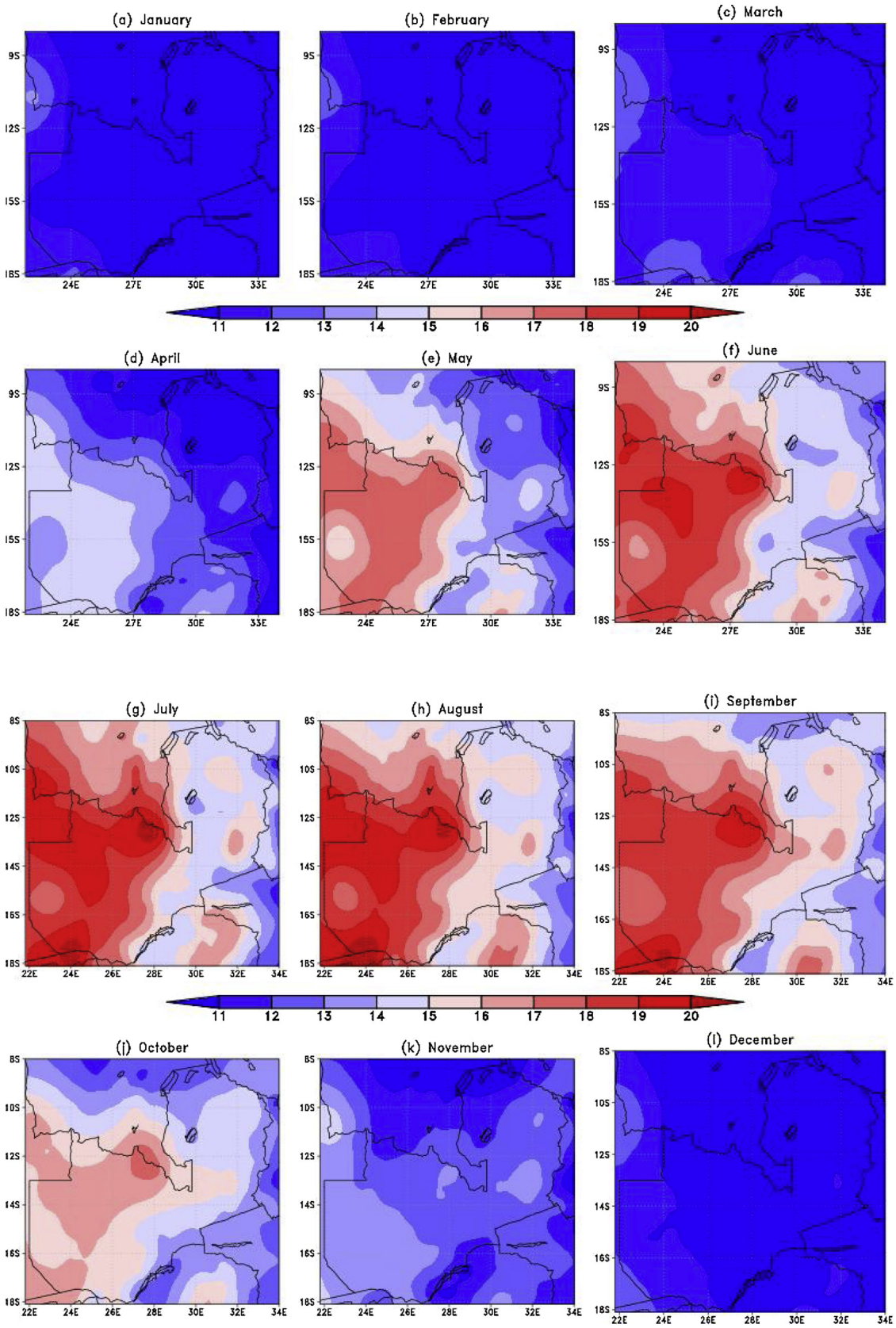

Fig. 2. Monthly climatology of DTR (°C) across Zambia during the period 1930–2016, averaged over longitudes 21.8–34 °E and latitudes 18 – 8 °S.

DTR values over much of the western half can be attributed to low rainfall and hence low cloud cover as compared to the eastern half of the country. This is further collaborated by the observation of dominant low DTR values during the months November – April which coincides with the rainy season over Zambia (Hachigonta et al., 2008; Libanda et al., 2015). During the rainy season, overcasts of low and mid-level stratocumuliform clouds are common across the country and they are often punctuated by heavy rainfall and thunderstorms. Clouds inherently enhance downwelling longwave radiation which increases Tmin while reflecting of sunlight reduces Tmax (Dai et al., 1999) thereby encouraging the plummeting of DTR.

In general, the highest DTR values are observed from May – September, a period generally characterized by clear skies. When compared to clear skies, clouds have been found to reduce DTR values by up to 50% (Braganza et al., 2004; Wang and Shilenje, 2017). Land use and land cover change (LUCC) also significantly contributes to DTR variability via changes in evapotranspiration (Wen-Jian and Hai-Shan, 2013). For instance, during May – September, most farm areas across Zambia are harvested hence the country is characterised by reduced land cover and therefore, high DTR values. In fact, LUCC has been reported to exert larger influence on DTR than on mean temperature (Wen-Jian and Hai-Shan, 2013).

Results presented in Fig. 2 are somewhat counterintuitive because most parts of Northwestern Province, a region known to experience high annual rainfall and cloud cover (Libanda et al., 2016a, 2016b), exhibits high DTR values. This single most striking observation confirms the effect of factors aside from cloudiness on DTR.

The dominant DTR patterns reported in Fig. 2 have the potential to transform the health sector of Zambia. For example, it is well established that low DTR values are associated with an increase in malaria cases (Wang and Shilenje, 2017); therefore, this information can be used by the health sector to plan the distribution of mosquito nets and to carry out health awareness campaigns. Advisory bulletins against exposure to high DTR can also widely be made available as it has been found that high DTR values aggravate cardiovascular diseases and encourage increased burden of premature death (Zhang et al., 2017).

Areas experiencing a warming tendency (Western half) in maximum compared to minimum temperatures need to be closely monitored as this can disrupt soil moisture and increase stress levels in plants thereby negatively affecting plant growth, flowering, maturity and ultimately yield (Sharma et al., 2018).

The results of the correlational analyses are shown in Fig. 3. Mean annual DTR is negatively correlated with mean annual cloud cover with a strong and statistically significant coefficient of -0.8 but its correlation with precipitation weakens to -0.5 at the α 0.05. This weakness can be explained by the fact that sometimes precipitation does not fall despite a cloudy celestial dome. This negative correlation can be attributed to the reduction of maximum temperatures with an increase in cloudiness. Similar results have been found in Europe (Jones, 1995), China (Xia, 2013) and recently, in East Africa (Wang and Shilenje, 2017).

The spatial seasonal evolution of DTR is presented in Fig. 4. Apart from parts of Senanga, Livingstone and surrounding areas, the rest of Zambia is characterized by low DTR ($<$ 11 °C) during the December – February (DJF) months. These results are not surprising considering that the Livingstone area is generally a semi-arid subtropical region. Although DJF is the core of the rainy season in Zambia (Libanda et al., 2016a, 2016b), the east-west pattern of DTR is again maintained here.

As the rainy season begins to withdraw during the months of March – May (MAM), high DTR values are seen to intensify and propagate eastwards (Fig. 4b). By June – August (JJA; Fig. 4c), the western half of the country generally experiences DTR values

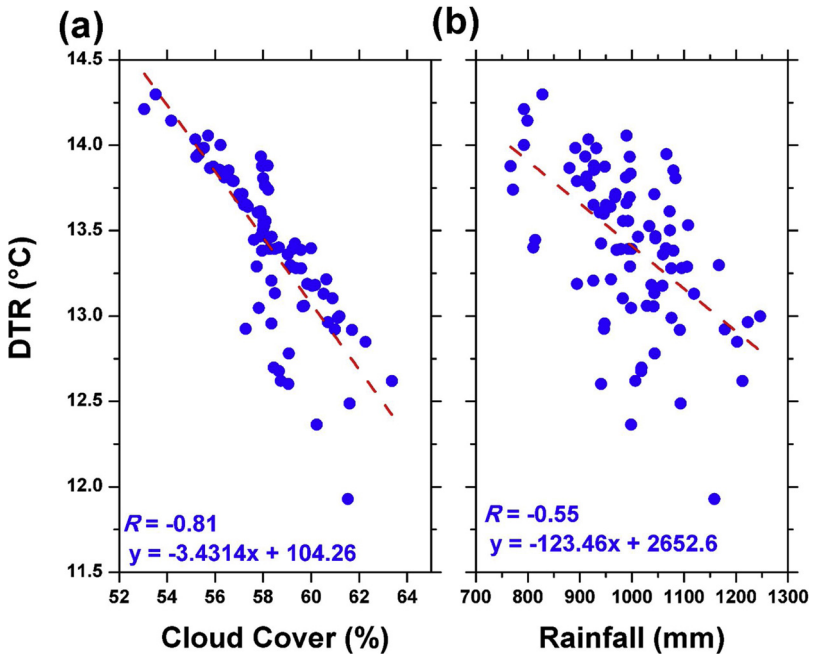

Fig. 3. Correlation between (a) mean annual DTR and mean cloud cover (b) mean annual DTR and mean annual precipitation across Zambia during the period 1930–2016 at 95% confidence level, averaged over longitudes 21.8–34 °E and latitudes 18 – 8 °S.

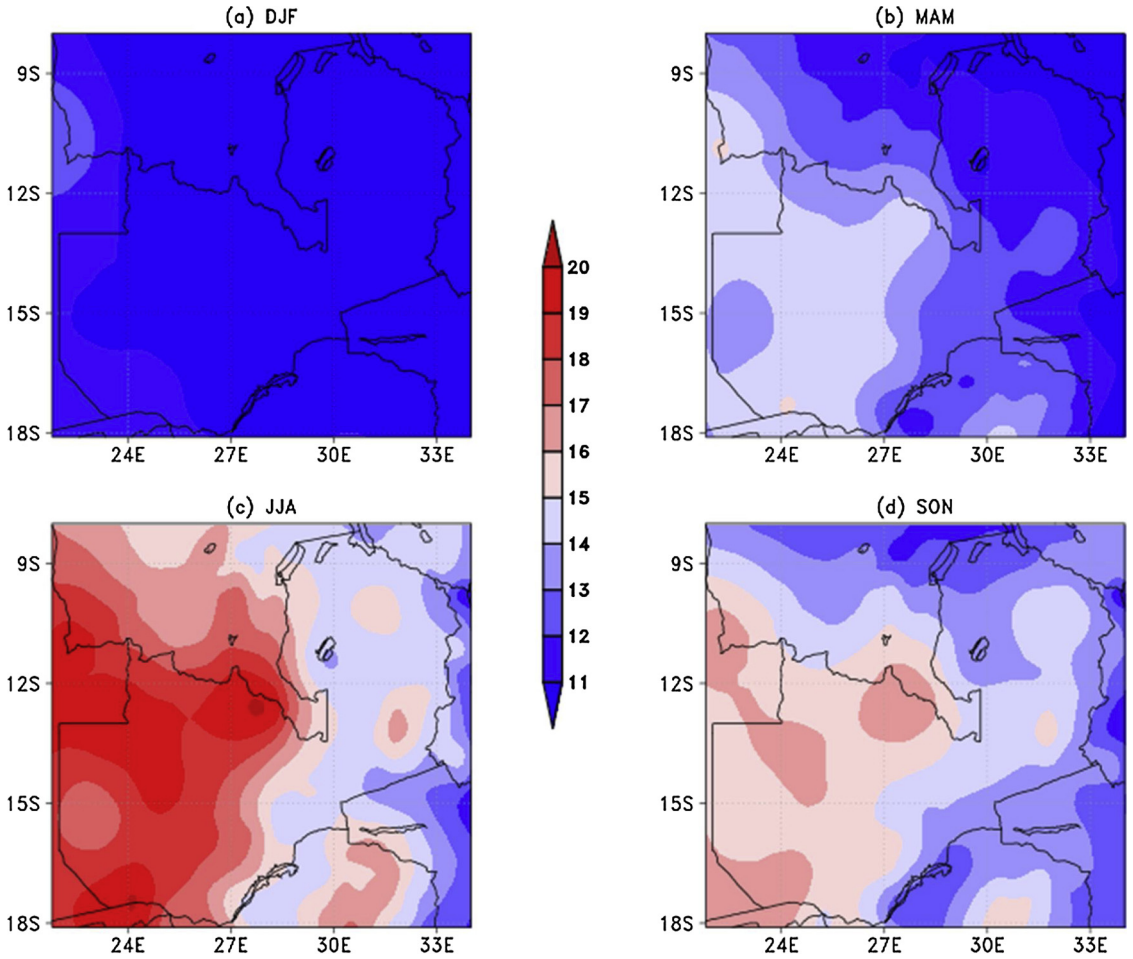

Fig. 4. seasonal evolution of DTR across Zambia during the period 1930–2016, averaged over longitudes 21.8–34 °E and latitudes 18 – 8 °S.

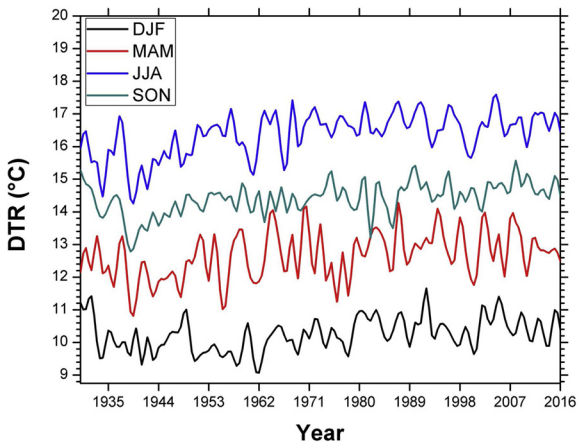

Fig. 5. Interannual variations of DTR across Zambia during the period 1930–2016; for: December – February (black), March – May (red), June – August (JJA) and, September – November (SON), averaged over longitudes 21.8–34 °E and latitudes 18 – 8 °S (For interpretation of the references to colour in this figure legend, the reader is referred to the web version of this article).

greater than 18 °C and this marks the season of the highest DTR values across Zambia. During September -October (SON; Fig. 4d), DTR begins to drop again just before a new rainy season is ushered in.

The interannual variability of DTR was investigated for each season. Results (Fig. 5) indicate that Zambia experiences the highest (lowest) DTR during JJA (DJF) throughout the study period (1930–2016). These results are in agreement with the observations made

Table 2
Statistical summary of Mann-Kendall trend test for seasonal variability of DTR in Zambia during the period 1930–2016, averaged over longitudes 21.8–34 °E and latitudes 18 – 8 °S. All the results were statistically significant at the 95% confidence level.

Metric	DJF	MAM	JJA	SON
n	87	87	87	87
Mean	10.2	12.6	16.4	14.4
Standard deviation	0.5	0.7	0.6	0.4
α	0.5	0.5	0.5	0.5
p-value	0.001	0.0008	3.091e-07	4.281e-06
Sen's slope	0.0016	0.0024	0.0033	0.0031
Significance	Significant	Significant	Significant	Significant

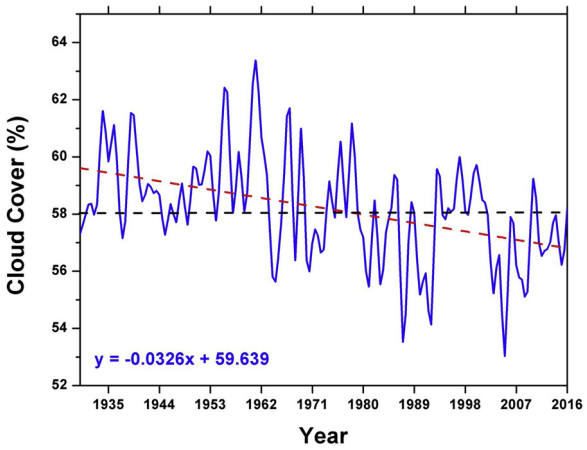

Fig. 6. Interannual variations of mean cloud cover over Zambia during the period 1930–2016, averaged over longitudes 21.8–34 °E and latitudes 18 – 8 °S. The black dashed line shows the average whereas the red dashed line shows the decreasing trend of cloud cover (For interpretation of the references to colour in this figure legend, the reader is referred to the web version of this article).

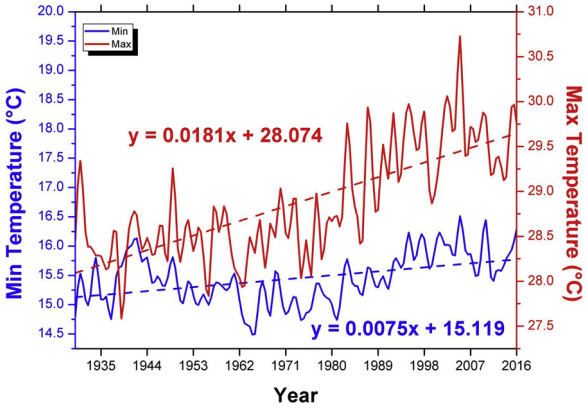

Fig. 7. Timeseries of minimum and maximum temperatures across Zambia during the period 1930–2016, averaged over longitudes 21.8–34 °E and latitudes 18 – 8 °S. The red (blue) dashed line shows the increasing trend of maximum (minimum) temperature (For interpretation of the references to colour in this figure legend, the reader is referred to the web version of this article).

under spatial analysis (Fig. 4) and with the expected climate of southern Africa (Reason, 2016).

Being a landlocked country, DTR across Zambia is rarely affected by ocean currents as compared to coastal areas e.g. Maputo in neighbouring Mozambique which is affected by the warming influence of the Agulhas Current (Reason, 2016). Cold and warm fronts also have very minimal effect on time-averaged DTR (Dai et al., 1999). Therefore, the variability of DTR across Zambia is mainly attributed to local forcing.

Results (Table 2) from the Mann-Kendall trend test shows marginal increments in DTR during all the seasons with JJA and SON being statistically significant at the α 0.05. The observed small increments can be attributed to a general decrease in precipitation (Libanda and Chilekana, 2018) and cloud cover over Zambia (Fig. 6).

It is worth noting that DTR varies markedly in space and time across the globe because different regions are affected by different

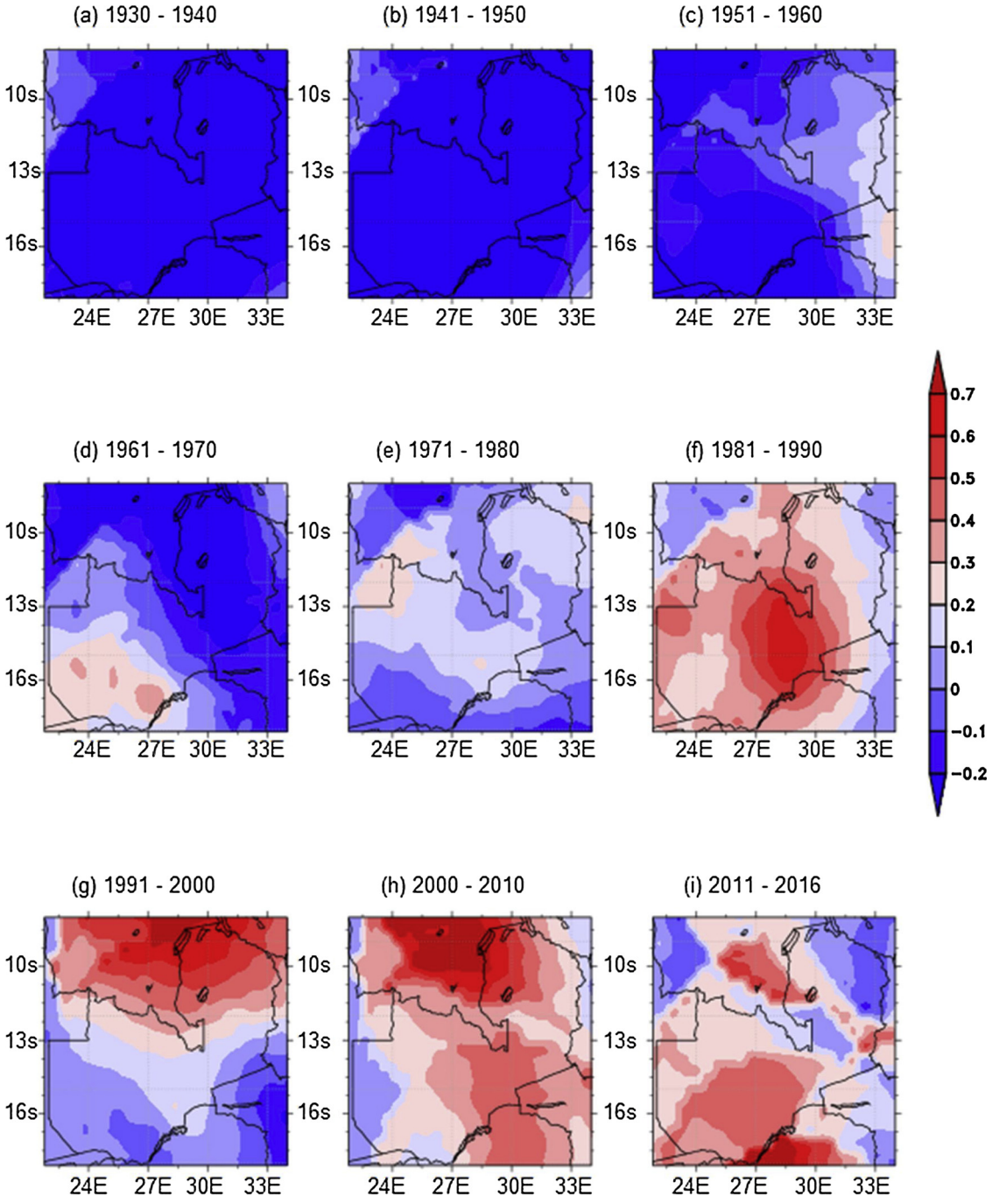

Fig. 8. Decadal DTR anomalies across Zambia during the period 1930–2016, averaged over longitudes 21.8–34 °E and latitudes 18 – 8 °S.

factors. Although there have been reports of marginal decrements in DTR in some regions, others have reported increments as is the case in this study. For example, increase in DTR has been reported in Europe (Makowski et al., 2009). Additionally, model simulations show an increase in DTR over central Asia during the summer months suggesting that maximum temperatures will have record-breaking increments compared to minimum temperatures during the 2050s (Gupta, 2005)

Changes in minimum (Tmin) and maximum (Tmax) temperatures were analysed (Fig. 7). Both Tmin and Tmax are exhibiting an upward trend especially beginning from the late (early) 70 s (80 s). Overall, Tmax is observed to increase faster than Tmin. This warming trend is subsequently seen in the marginal DTR increments that have been reported in Table 2. In contrast, regions that have reported decrements in DTR have also observed that minimum temperatures are rising faster than maximum temperatures (Ongoma et al., 2013).

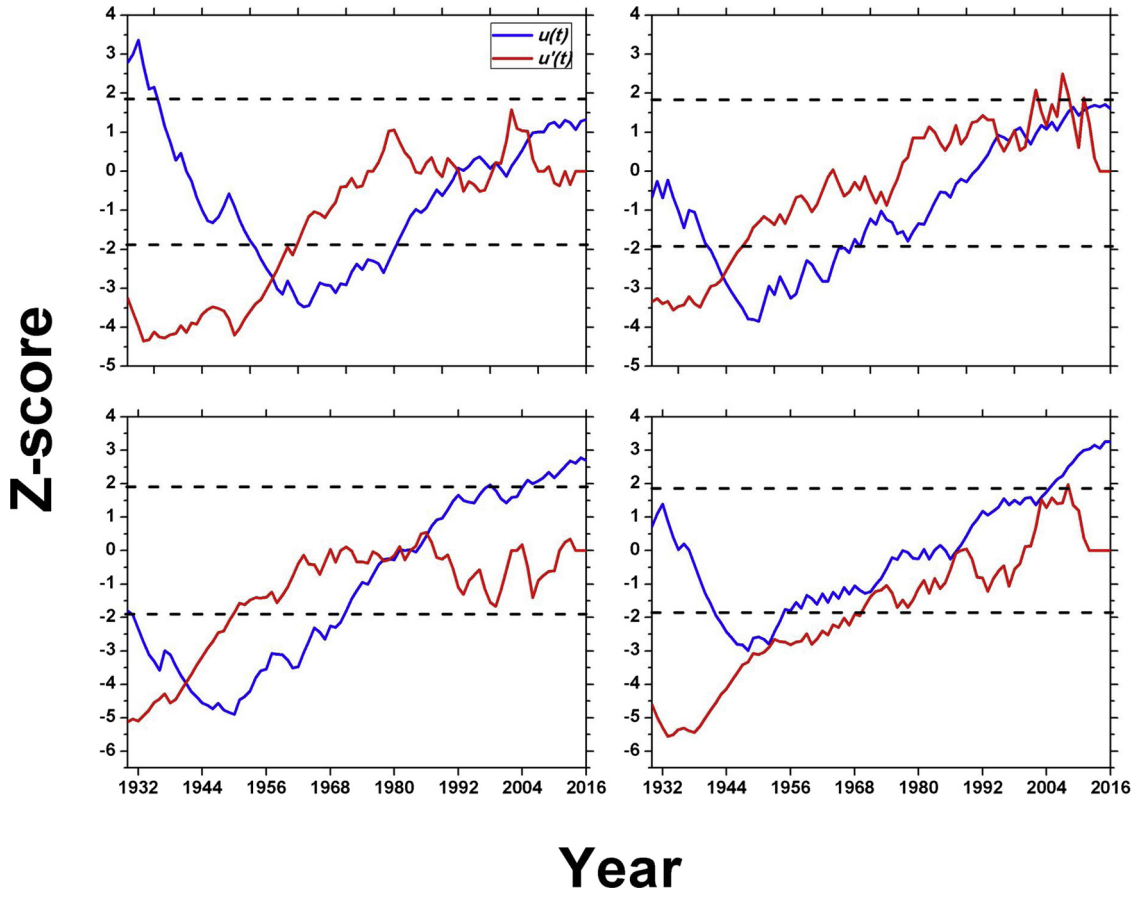

Fig. 9. Abrupt change in DTR trend across Zambia based on Sequential Mann-Kendal test statistic; where *u(t)* is forward sequential statistic and *u'(t)* is backward sequential statistic, for **(a)** DJF **(b)** MAM **(c)** JJA and **(d)** SON. The upper and lower dashed lines represent the confidence limits at $\alpha = 0.05$.

Decadal DTR anomalies are presented in Fig. 8. The highest warming rate was reported during the two consecutive decades from 1930–1950. This can be deduced from the fact that the two decades were characterized by the lowest DTR anomalies, typically below 0 °C over the whole country. On the other hand, 2000–2010 was the coolest decade of the study period and this is shown by the fact that it had the highest DTR anomalies.

Having observed an upward trend in DTR across the whole country (Table 2), sequential Mann-Kendall test was employed to investigate any sudden changes. Results (Fig. 9) indicate a decrease in DTR from the 1930s to the 1940s when an upward trend is observed across all seasons again. After the 1940s, DTR begun rising and this upward trend was statistically significant most of the time. Statistically significant abrupt changes were observed in the early 1990s across all seasons although these were short lived.

4. Concluding remarks

Returning to the aim set at the beginning of this study, it is now possible to state that there are increments of DTR across all seasons howbeit marginal. This trend is a result of a general reduction in cloud cover which correlates strongly with DTR with a statistically significant negative coefficient of -0.8. Results further indicate a dominant east-west pattern with higher DTR values being observed in the western half of the country. Although there are noticeable differences in the amplitude from one month to the other, this east-west pattern is persistent throughout all the months. Some surprising results include the observation that Northwestern Province, a region known to experience high annual rainfall and cloud cover (Libanda et al., 2016a, 2016b), exhibits high DTR values. This single most striking observation confirms the effect of factors aside from cloudiness on DTR in Zambia. There is therefore need for concerted research effort that will build on the findings embodied in this work to identify individual factors that explain the variance in DTR over Zambia.

Competing interests

The authors have no competing interests to declare

Acknowledgements

The first author carried out this work while on a PhD scholarship sponsored by the University of Edinburgh; the university is hereby acknowledged. The Climatic Research Unit of the University of East Anglia is acknowledged for the datasets used in this study. The Editor and the anonymous Reviewers are acknowledged for the comments that helped to improve this work.

References

Awange, J.L., Ferreira, V.G., Forootan, E., Khandu Andam-Akorful, S.A., Agutu, N.O., He, X.F., 2016. Uncertainties in remotely sensed precipitation data over Africa. Int. J. Climatol. 36 (1), 303–323. https://doi.org/10.1002/joc.4346.

Braganza, K., Karoly, D.J., Arblaster, J.M., 2004. Diurnal temperature range as an index of global climate change during the twentieth century. Geophys. Res. Lett. 31 (13), 2–5. https://doi.org/10.1029/2004GL019998.

Collatz, G.J., Bounoua, L., Los, S.O., Randall, D.A., Fung, I.Y., Sellers, P.J., 2000. A mechanism for the influence of vegetation on the response of the diurnal temperature range to changing climate. Geophys. Res. Lett. 27 (20), 3381–3384. https://doi.org/10.1029/1999GL010947.

Dai, A., Trenberth, K.E., Karl, T.R., 1999. Effects of clouds, soil moisture, precipitation, and water vapor on diurnal temperature range. J. Clim. 12 (8), 2451–2473.

Gupta, K.R., 2005. Global Warming: Problems and Policies. Atlantic Publishers.

Hachigonta, S., Reason, C.J.C., Tadross, M., 2008. An analysis of onset date and rainy season duration over Zambia. Theor. Appl. Climatol. 91 (1–4), 229–243. https://doi.org/10.1007/s00704-007-0306-4.

Harris, I., Jones, P.D., Osborn, T.J., 2014. Updated high-resolution grids of monthly climatic observations – the CRU TS3.10 dataset. Int. J. Climatol. 34 (3), 623–642. https://doi.org/10.1002/joc.3711.

Hastings, D.A., Paula, K.D., 1999. Global Land one-kilometer base elevation (GLOBE) digital elevation model, documentation, volume 1.0. Key to Geophysical Records Documentation (KGRD). Boulder.

IPCC, 2001. Climate Change: The Scientific Basis. Contribution of Working Group 1 to the Third Assessment Report of the Intergovernmental Panel on Climate Change. Cambridge University Press.

IPCC, 2007. Climate change 2007: an assessment of the intergovernmental panel on climate change. Change 446 (November), 12–17. https://doi.org/10.1256/004316502320517344.

Jones, P.D., 1995. Maximum and minimum temperature trends in Ireland, Italy, Thailand, Turkey and Bangladesh. Atmos. Res. 37 (1–3), 67–78. https://doi.org/10.1016/0169-8095(94)00069-P.

Kalnay, E., Cai, M., 2003. Impact of urbanization and land-use change on climate. Nature 423 (6939), 528–531. https://doi.org/10.1038/nature01675.

Karl, T.R., Kukla, G., Razuvayev, V.N., Changery, M.J., Quayle, R.G., Heim, R., Fu, C., 1991. Global warming: evidence for asymmetric diurnal temperature change. Geophys. Res. Lett. 18 (12), 2253–2256. https://doi.org/10.1029/91GL02900.

Kendall, M.G., 1975. Rank Correlation Methods, 4th edn. London.

Lauritsen, R.G., Rogers, J.C., 2012. U.S. Diurnal temperature range variability and regional causal mechanisms, 1901–2002. J. Clim. 25 (20), 7216–7231. https://doi.org/10.1175/JCLI-D-11-00429.1.

Libanda, B., Chilekana, N., 2018. Projection of frequency and intensity of extreme precipitation in Zambia: a CMIP5 Study. Clim. Res. 76, 59–72.

Libanda, B., Nkolola, B., Musonda, B., 2015. Rainfall variability over Northern Zambia. J. Sci. Res. Rep. 6 (6), 416–425. https://doi.org/10.9734/JSRR/2015/16189.

Libanda, B., Allan, D., Banda, N., Luo, W., Chilekana, N., Nyasa, L., 2016a. Predictor selection associated with statistical downscaling of precipitation over Zambia. Asian J. Phys. Chem. Sci. 1 (2), 1–9. https://doi.org/10.9734/AJOPACS/2016/31545.

Libanda, B., Ogwang, B.A., Ongoma, V., Chilekana, N., Nyasa, L., 2016b. Diagnosis of the 2010 DJF flood over Zambia. Nat. Hazards 81 (1), 189–201. https://doi.org/10.1007/s11069-015-2069-z.

Libanda, B., Zheng, M., Chilekana, N., 2018. Spatial and temporal patterns of drought in Zambia. J. Arid Land In press.

Makowski, K., Jaeger, E.B., Chiacchio, M., Wild, M., Ewen, T., Ohmura, A., 2009. On the relationship between diurnal temperature range and surface solar radiation in Europe. J. Geophys. Res. Atmos. 114 (7), 1–16. https://doi.org/10.1029/2008JD011104.

Mann, H., 1945. Non-parametric tests against trend. Econometrica 13, 245–259.

Ongoma, V., Muthama, J.N., Gitau, W., 2013. Evaluation of urbanization on urban temperature of Nairobi City. Kenya. Global Meteorology 2 (e1), 1–5. https://doi.org/10.4081/gm.2013.e1.

Ongoma, V., Chen, H., Gao, C., Sagero, P.O., 2017. Variability of temperature properties over Kenya based on observed and reanalyzed datasets. Theor. Appl. Climatol. 1–16. https://doi.org/10.1007/s00704-017-2246-y.

Pearson, K., 1895. Notes on regression and inheritance in the case of two parents. Proc. R. Soc. London 58, 240–242.

Qu, M., Wan, J., Hao, X., 2014. Analysis of Diurnal Air Temperature Range Change in the Continental United States. https://doi.org/10.1016/j.wace.2014.05.002.

Reason, C., 2016. Climate of Southern Africa. https://doi.org/10.1093/acrefore/9780190228620.013.513.

Sen, P.K., 1985. Estimates of the regression coefficient based on Kendall's Tau. J. Am. Stat. Assoc. 6341128116 (1977), 203–208. Retrieved from. http://www.jstor.org/stable/2285891.

Sharma, P.J., Loliyana, V.D., Resmi, S.R., Timbadiya, P.V., Patel, P.L., 2018. Spatiotemporal trends in extreme rainfall and temperature indices over Upper Tapi Basin. India. Theoretical and Applied Climatology 134 (3–4), 1329–1354. https://doi.org/10.1007/s00704-017-2343-y.

Sneyers, R., 1990. On the Statistical Analysis of Series of Observations. WMO Tech. Note No. 143. Genève: Secretariat of the World Meteorological Organization, Geneve.

Sun, D., Pinker, R.T., Kafatos, M., 2006. Diurnal temperature range over the United States: a satellite view. Geophys. Res. Lett. 33 (5), 2–5. https://doi.org/10.1029/2005GL024780.

Wang, Y., Shilenje, W.Z., 2017. Variability of diurnal temperature range in East Africa during 1921–2010. J. Trop.l Meteorol. 23 (December), 1–14.

Wen-Jian, H., Hai-Shan, C., 2013. Impacts of regional-scale land Use/Land cover change on diurnal temperature range. Adv. Clim. Chang. Res. 4 (3), 166–172. https://doi.org/10.3724/SP.J.1248.2013.166.

Xia, X., 2013. Variability and trend of diurnal temperature range in China and their relationship to total cloud cover and sunshine duration. Ann. Geophys. 31 (5), 795–804. https://doi.org/10.5194/angeo-31-795-2013.

Zhang, Y., Yu, C., Yang, J., Zhang, L., Cui, F., 2017. Diurnal temperature range in relation to daily mortality and years of life lost in Wuhan, China. Int. J. Environ. Res. Public Health 14 (8), 1–11. https://doi.org/10.3390/ijerph14080891.